

1 **Impact of ~~burial~~occurrence conditions on NO₃⁻-N source apportionment in**
2 **groundwater: Insights from PCA-APCS-MLR and MixSIAR methods**

3 Yang Liu^{1,2,3}, Jian Luo⁴, Yajie Wu⁵, Ziyang Zhang^{1,2,3}, Xilai Zheng^{1,2,3}, Tianyuan
4 Zheng^{1,2,3*}

5 1. College of Environmental Science and Engineering, Ocean University of China,
6 Qingdao 266100, China

7 2. Shandong Provincial Key Laboratory of Marine Engineering Geology and the
8 Environment, Ocean University of China, Qingdao 266100, China

9 [3. Key Laboratory of Marine Environment and Ecology, Ministry of Education, Ocean](#)
10 [University of China, Qingdao 266100, China](#)

11 [34. School of Civil and Environmental Engineering, Georgia Institute of Technology,](#)
12 [Atlanta, GA 30332, USA](#)

13 [45. College of Engineering, Ocean University of China, Qingdao 266100, China](#)
14

15 **Corresponding author:**

16 Tianyuan Zheng

17 E-mail: zhengtianyuan@ouc.edu.cn
18

19 **Abstract**

20 [Nitrate-N \(NO₃⁻-N\)](#) contamination in groundwater poses a significant threat to
21 drinking water safety and ecosystem health, with accurate source identification being
22 crucial for effective pollution control. Previous studies on NO₃⁻-N source
23 apportionment in groundwater have largely neglected ~~aquifer~~[groundwater](#)
24 ~~burial~~[occurrence](#) conditions. In this study, groundwater samples from aquifers with
25 ~~varying~~[different](#) ~~burial~~[occurrence](#) conditions were collected and analyzed using an
26 integrated approach combining hydrochemical analysis (PCA-APCS-MLR) and stable
27 isotope mixing modeling (MixSIAR) to identify and quantify NO₃⁻-N pollution sources.
28 The results demonstrate that NO₃⁻-N concentrations in 75% of the groundwater samples

29 exceeded the standard for drinking water quality of China ($\leq 10 \text{ mg N L}^{-1}$)WHO
30 ~~drinking water standard~~. NO_3^- -N in unconfined groundwater predominantly originates
31 from soil nitrogen (58%), with a non-negligible contribution from chemical fertilizers.
32 NO_3^- -N enrichment in confined groundwater is primarily attributed to manure &
33 sewage (37.9%). PCA-APCS-MLR analysis revealed that the dominant NO_3^- -N sources
34 in unconfined groundwater and confined groundwater were chemical fertilizers (52.5%)
35 and manure & sewage (53.9%), respectively. The MixSIAR model further identified
36 soil nitrogen (58%) and manure & sewage (37.9%) as the primary contributors to NO_3^-
37 -N in unconfined and confined groundwater, respectively. These findings suggest that
38 unconfined groundwater in regions with high soil nitrogen reserves is at persistent risk
39 of NO_3^- -N contamination. In addition, ignoring the groundwater occurrence conditions
40 leads to marked deviations in the source apportionment results derived from both the
41 PCA-APCS-MLR and MixSIAR approaches. ~~neglecting aquifer burial groundwater~~
42 ~~occurrence conditions would introduce absolute errors of 22%–24% in source~~
43 ~~apportionment results obtained from both PCA-APCS-MLR and MixSIAR approaches.~~
44 This study highlights that considering the occurrence conditions serves as a key
45 indicator for distinguishing the primary sources of NO_3^- -N in groundwater, which can
46 ~~aquifer confinement must be rigorously considered as a critical factor in NO_3^- -N source~~
47 ~~identification and pollution control strategies to~~ enhance the accuracy of source
48 apportionment and the effectiveness of management measures.

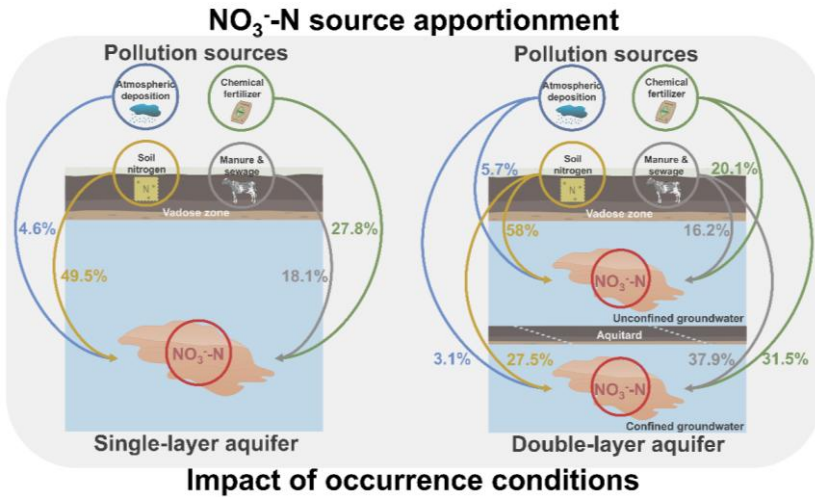
49 **Keywords:** Groundwater; occurrence conditions; NO_3^- -N ~~pollution~~; ~~S~~source
50 apportionment; PCA-APCS-MLR; MixSIAR

51

设置了格式: 字体: 非加粗

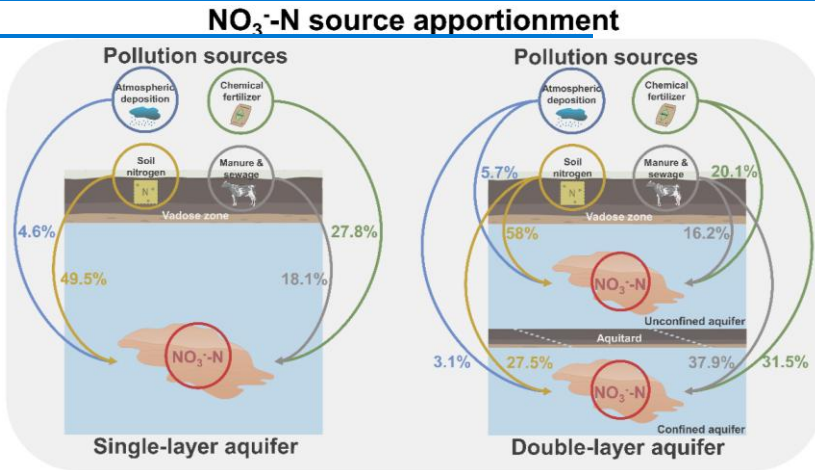
设置了格式: 上标

52 Graphical Abstract



带格式的: 正文, 居中

53 Impact of occurrence conditions



54 Impact of burial conditions

55

56 Highlights

- 57 • Elucidated the sources of NO₃⁻-N in aquifers groundwater under different
- 58 burial occurrence conditions.
- 59 • Soil nitrogen contributes over 50% to the NO₃⁻-N in the unconfined
- 60 aquifer groundwater.
- 61 • NO₃⁻-N in confined aquifer groundwater mainly originates from manure & sewage.

62 • Neglecting occurrence conditions leads to significant deviations in source
63 apportionment. Source apportionment results have an error of 24% without considering
64 the burial occurrence conditions.

65

66 1. Introduction

67 Groundwater ~~N~~nitrate-N (NO_3^- -N) contamination has persisted for nearly a century
68 worldwide, emerging as a critical environmental challenge that threatens both human
69 health and ecological security (Xin et al., 2019). As a highly toxic pollutant, NO_3^- -N
70 poses significant health risks including methemoglobinemia and cancer when ingested
71 through drinking water (Picetti et al., 2022), especially particularly when its
72 concentrations exceeds the WHO drinking water standards safe limit of 11.3 mg N L⁻¹.

设置了格式: 字体: (默认) Times New Roman

73 It also causes severe ecological impacts such as aquatic eutrophication, primarily
74 through groundwater discharge into rivers, lakes, and coastal waters (Romanelli et al.,
75 2020). As a highly toxic pollutant, NO_3^- -N poses significant health risks including
76 methemoglobinemia and cancer when ingested through drinking water (Picetti et al.,
77 2022), while also causing severe ecological impacts such as aquatic eutrophication
78 (Romanelli et al., 2020). The environmental persistence of NO_3^- -N is exacerbated by

设置了格式: 字体: (默认) Times New Roman

79 limited natural attenuation in groundwater systems due to weak denitrification
80 processes, resulting in long-term accumulation of NO_3^- -Nthis contaminant (Rivett et al.,
81 2008). The primary sources of NO_3^- -N include non-point source pollution from
82 agricultural activities (fertilizer application and livestock operations) and point source
83 pollution from industrial effluents and domestic sewage (Xin et al., 2021).

设置了格式: 字体: (默认) Times New Roman

84 Consequently, the accurate identification and dissection of NO_3^- -N pollution sources
85 are pivotal to the assessment and control of groundwater pollution risks. Despite some
86 advancements in NO_3^- -N source apportionment over the past decades (Yang et al., 2013;
87 Gibrilla et al., 2020), the majority of studies have overlooked the burial occurrence
88 conditions and stratigraphic characteristics of unconfined and confined
89 aquifers groundwater. Ignoring this issue can lead to inaccurate source apportionment

90 results, and consequently affect the scientific nature and effectiveness of groundwater
91 pollution prevention and control strategies.

92 Current studies on NO_3^- -N source apportionment in groundwater predominantly
93 simplifies complex multi-layer aquifer systems into single-layer models ~~without~~
94 ~~accounting for differences in burial occurrence conditions~~ (Yu et al., 2020). While this
95 simplification facilitates analysis, it introduces substantial limitations due to
96 fundamental differences between unconfined and confined aquifers in terms of recharge
97 mechanisms, flow paths, hydraulic characteristics, and contaminant transport behavior
98 (Liang et al., 2017). Unconfined aquifers, characterized by strong connectivity with
99 surface water, are highly vulnerable to anthropogenic activities (e.g., agricultural
100 fertilization, industrial effluents, and domestic sewage), allowing contaminants to
101 readily leach into groundwater through precipitation or surface runoff, resulting in rapid
102 NO_3^- -N accumulation that typically reflects recent pollution caused by recent human
103 activities (Gutiérrez et al., 2018). In contrast, confined aquifers, protected by overlying
104 aquitards, exhibit slower contaminant migration, with NO_3^- -N pollution often
105 representing legacy effects from historical agricultural practices (Wong et al., 2015).
106 ~~Failure to differentiate these aquifer types may lead to biased source contribution~~
107 ~~assessments.~~ In addition, the transformation rates of nitrogen components from
108 different pollution sources vary in aquifers with different burial occurrence conditions.
109 Unconfined aquifers are generally aerobic environments, where the mineralization and
110 nitrification of organic nitrogen occur rapidly, leading to a swift increase in NO_3^- -N
111 concentration (Liu et al., 2022). In contrast, confined aquifers tend to have reducing
112 conditions, which restrict the nitrogen transformation rate and cause a lag in NO_3^- -N
113 formation (Ma et al., 2019). As a result, the source of NO_3^- -N may be mistakenly
114 attributed to other pollution sources. ~~Therefore, elucidating the sources of NO_3^- -N~~
115 ~~pollution in actual double-layered aquifers groundwater with different burial occurrence~~
116 ~~conditions and revealing the discrepancies between these results and those obtained~~
117 ~~without considering burial occurrence conditions can provide a more accurate basis for~~

118 [groundwater NO₃⁻-N pollution risk assessment.](#)

119 In recent years, some progress has been made in the identification of NO₃⁻-N
120 pollution sources in groundwater through the application of hydrochemical analysis
121 methods and stable isotope mixing models (Minet et al., 2017; Yu et al., 2022).
122 Hydrochemical analysis methods mainly include ion ratio methods, hydrochemical
123 diagram methods, and quantitative hydrochemical analysis methods. Among these,
124 quantitative hydrochemical analysis is the core, which encompasses models such as the
125 chemical mass balance (CMB), positive matrix factorization (PMF), and multivariate
126 statistical models (e.g., principal component analysis and multiple linear regression
127 analysis). Among these methods, the absolute principal component score-multiple
128 linear regression (APCS-MLR) method has garnered considerable attention due to its
129 high efficiency and broad applicability (Meng et al., 2018; Ruan et al., 2024). APCS-
130 MLR can extract key pollution source information by reducing data redundancy
131 through principal component analysis while retaining the essential characteristics of
132 major pollution sources. Additionally, APCS-MLR can establish a quantitative
133 relationship between principal component scores and actual pollutant concentrations
134 via multiple linear regression, thereby accurately calculating the contribution rates of
135 various pollution sources. Subsequently, stable isotope techniques have been applied in
136 the identification of NO₃⁻-N pollution sources in groundwater. The development of this
137 technology in groundwater NO₃⁻-N source apportionment has evolved from the use of
138 single isotopes ($\delta^{15}\text{N}$) to the combined application of multiple isotopes (both $\delta^{15}\text{N}$ and
139 $\delta^{18}\text{O}$) (Kellman and Hillaire-Marcel, 2003; Ji et al., 2022). By analyzing the isotopic
140 compositions of nitrogen ($\delta^{15}\text{N}$) and oxygen ($\delta^{18}\text{O}$) in NO₃⁻-N, this technique can
141 effectively distinguish different sources of NO₃⁻-N pollution in groundwater (such as
142 agricultural fertilization, domestic sewage, soil nitrogen, and atmospheric deposition)
143 (Ransom et al., 2016), thereby providing an important supplement to traditional
144 hydrochemical analysis methods. To further quantify the contribution proportions of
145 different pollution sources and enhance the accuracy of source identification, the stable

146 isotope mixing model based on the R language, MixSIAR, has been developed. The
147 MixSIAR method, by integrating isotope data with prior information (the ranges of
148 isotopic values and initial estimates of their contributions) on pollution sources, is
149 capable of quantifying the relative contributions of different pollution sources and
150 assessing the uncertainty of the results. For example, Mao et al. (2023) used the
151 MixSIAR method to analyze the distribution of NO₃⁻-N pollution sources in the
152 groundwater of Poyang Lake, China, revealing that manure & sewage accounted for
153 52%, chemical fertilizers for 17%, and soil nitrogen for 21.5% of the pollution sources.
154 In this study, hydrochemical analysis methods and the MixSIAR method were
155 employed to comprehensively identify the ~~sources of~~ NO₃⁻-N pollution sources in
156 ~~aquifers groundwater~~ under different ~~burial occurrence~~ conditions.

设置了格式: 字体: 非加粗

157 ~~The Old County groundwater source area is a vital water supply hub in the central~~
158 ~~region of Shandong Province. However, with the development of industry and~~
159 ~~agriculture and the increasing level of urbanization, the Old County source area is~~
160 ~~facing severe NO₃⁻-N contamination in groundwater. Identifying the sources of NO₃⁻-~~
161 ~~N in aquifers under different burial conditions in this region is crucial for elucidating~~
162 ~~the genesis of “high nitrogen groundwater”. In this study, To bridge the methodological~~
163 ~~gap associated with overlooking groundwater occurrence conditions in NO₃⁻-N source~~
164 ~~apportionment and to elucidate the genesis of “high-nitrogen groundwater” in the Old~~
165 ~~County groundwater source area, this study undertook an integrated field campaign and~~
166 ~~laboratory analysis.~~ Groundwater samples were collected from 64 wells, and soil,
167 fertilizer, manure, and precipitation samples were also gathered within the study area.
168 The water chemistry indicators and isotopic characteristics of these samples were
169 analyzed. Subsequently, PCA-APCS-MLR and MixSIAR methods were employed for
170 data analysis. The objectives of this study are (1) to quantify the concentration and
171 distribution of NO₃⁻-N in groundwater within the study area; (2) to quantitatively
172 identify the sources of NO₃⁻-N contamination in ~~aquifers groundwater~~ under different
173 ~~burial occurrence~~ conditions using hydrochemical analysis and the MixSIAR method;

带格式的: 孤行控制

174 and (3) ~~to clarify distinct NO₃⁻-N pollution sources in confined and unconfined~~
175 ~~groundwater, highlighting the critical role of occurrence conditions for targeted~~
176 ~~management to define the error in the analysis of groundwater NO₃⁻-N sources~~
177 ~~apportionment without considering burial occurrence conditions. We hypothesize that~~
178 ~~the primary sources of NO₃⁻-N pollution differ significantly between unconfined and~~
179 ~~confined aquifers groundwater, and neglecting groundwater occurrence conditions will~~
180 ~~introduce a discrepancy in the results of quantitative NO₃⁻-N source apportionment. The~~
181 study aims to provide a more accurate basis for assessing the risk of NO₃⁻-N
182 contamination in regional groundwater.

设置了格式: 字体: 非加粗
设置了格式: 字体: 非加粗
设置了格式: 字体: 非加粗
设置了格式: 字体: 非加粗

183

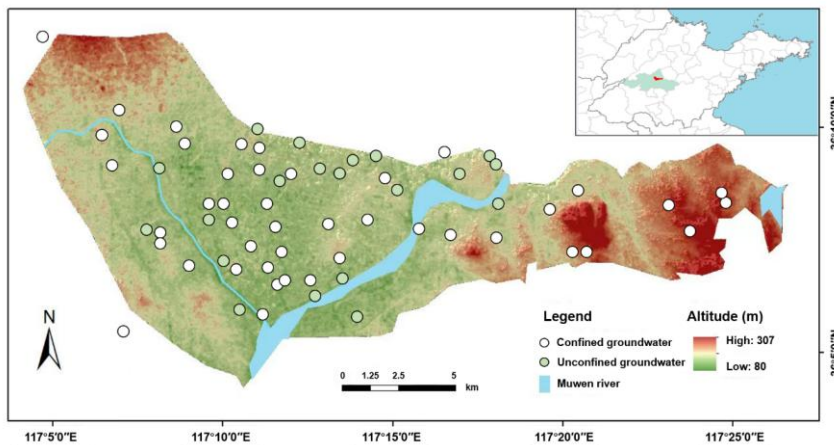
184 2. Materials and methods

185 2.1 Study region

186 The study area is located on the western edge of the Tai-Lai Basin in the lower
187 reaches of the Yellow River (Fig.1), to the east of Tai'an urban area (117°04'09"E–
188 117°26'45"E, 36°04'16"N–36°12'10"N), with a total area of approximately 220 km².
189 The topography is characterized as a proluvial and alluvial plain at the foot of Mount
190 Tai, with an overall terrain slope from the northwest to the southeast. The study area
191 falls within the temperate continental semi-humid monsoon climate zone, featuring hot
192 and rainy summers, as well as cold and dry winters. The average annual temperature is
193 12.9°C, and the average annual precipitation is 790.69 mm. Precipitation exhibits
194 significant spatiotemporal variability, with uneven seasonal distribution and large
195 interannual fluctuations. The primary aquifer formations in the study area consist of
196 two types: the Quaternary unconsolidated porous aquifer group and the Cambrian-
197 Ordovician carbonate rock fracture karst aquifer group. The former is mainly composed
198 of medium to coarse sand, with recharge primarily from atmospheric precipitation and
199 infiltration of surface water, and discharge through evaporation, artificial extraction,
200 replenishment of surface water, and inter-aquifer flow to other aquifers. The latter is
201 mostly situated beneath the Quaternary strata, with recharge mainly from "skylight"

设置了格式: 字体: 非加粗

202 recharge of Quaternary water and lateral flow recharge from regional bedrock fracture
203 aquifers, and discharge through artificial extraction, runoff discharge, and upward
204 replenishment to the Quaternary porous water. The urban population in the study area
205 is approximately 28,000, with over 85% of the population engaged in agriculture and
206 animal husbandry.



207
208 **Fig.1.** Location of the Tailai Basin in lower reaches of the Yellow River and sampling sites in the
209 study region.

210 2.2 Sample collection

211 A total of 64 groundwater samples were collected from the study area. Prior to
212 sampling, wells were thoroughly flushed, and samples were taken from a depth of more
213 than 0.5 m below the groundwater table. For sealed wells, water stored in the pumping
214 pipe was completely drained before sampling. After collection, groundwater samples
215 were filtered through a 0.45 μm membrane filter and stored in 500 mL amber glass
216 bottles, which were then sealed and transported to the laboratory for refrigeration at
217 4°C. Groundwater samples intended for isotopic analysis were filtered through a 0.22
218 μm membrane filter and stored frozen in 50 mL polyethylene bottles. Five atmospheric
219 precipitation samples were collected using stainless-steel precipitation samplers. For
220 single-day precipitation events, one complete-event sample was collected, while for
221 multi-day precipitation events, samples were collected at 24-hour intervals. All

222 precipitation samples were stored in polyethylene bottles. Five typical fertilizer samples
223 (including urea and compound fertilizers) were collected based on local farmers'
224 fertilization practices. Given the difficulty in distinguishing between manure & sewage
225 pollution sources using $\delta^{15}\text{N}$ and $\delta^{18}\text{O}$ isotopes, these two sources were combined into
226 one category in this study. A total of 10 samples (including cow manure, pig manure,
227 chicken manure, sheep manure, goose manure, and sewage) were collected. Manure
228 samples were air-dried for later use, while sewage samples were filtered through a 0.22
229 μm membrane filter and stored frozen. Additionally, 20 agricultural soil samples were
230 collected using the plum blossom point layout method. Each sample was composed of
231 a mixture from 5 to 15 sampling points at a depth of 30 cm, with all sampling points
232 avoiding fertilized areas. The collected soil samples were thoroughly mixed after
233 removing roots and gravel and then stored.

234 2.3 Sample Analysis

235 ~~The concentration of NO_3^- -N was determined using ultraviolet spectrophotometry.~~
236 ~~The concentrations of K^+ , Na^+ , Ca^{2+} , Mg^{2+} , Cl^- , and SO_4^{2-} were measured using an ion~~
237 ~~chromatograph (ICS-3000, Dionex, USA), the concentration of HCO_3^- was determined~~
238 ~~by acid-base titration.~~

239 The concentration of NO_3^- -N was determined using the ultraviolet
240 spectrophotometric method (at 220 nm and 275 nm) following filtration through a 0.45
241 μm membrane. The concentrations of major ions (K^+ , Na^+ , Ca^{2+} , Mg^{2+} , Cl^- , and SO_4^{2-})
242 were measured using an ion chromatograph (ICS-3000, Dionex, USA). The separation
243 was achieved with an IonPac AS23 analytical column and an AG23 guard column,
244 using a carbonate eluent. The concentration of HCO_3^- was determined by acid-base
245 titration with a standardized HCl solution (0.02 M) to a bromocresol green-methyl red
246 endpoint. All analyses of water quality indicators adhered to standard methods
247 (Greenberg et al., 2005).

248 ~~For liquid samples (groundwater, atmospheric precipitation, and sewage) In the~~
249 ~~analysis of isotopic samples, $\delta^{15}\text{N}$ and $\delta^{18}\text{O}$ were measured using the azide reduction~~

设置了格式: 下标

设置了格式: 上标

设置了格式: 上标

设置了格式: 上标

设置了格式: 上标

设置了格式: 下标

设置了格式: 上标

设置了格式: 字体: (默认) Times New Roman, 字体颜色: 自动设置, 图案: 清除

设置了格式: 字体: (中文) + 中文正文 (等线), 字体颜色: 自动设置

250 method [for liquid samples \(groundwater, atmospheric precipitation, and sewage\)](#). This
251 involved chemically reducing NO_3^- -N in the samples to N_2O , which was then analyzed
252 using an elemental analyzer coupled with an isotope ratio mass spectrometer (Vario
253 Isotope Cube - Isoprime, Elementar) to obtain the isotopic values of $\delta^{15}\text{N}$ and $\delta^{18}\text{O}$. For
254 solid samples (soil, fertilizer, and manure), $\delta^{15}\text{N}$ and $\delta^{18}\text{O}$ were measured using the
255 high-temperature oxidation method. This procedure involved weighing an appropriate
256 amount of thoroughly ground powder sample, encapsulating it in a tin cup, and
257 analyzing it using an elemental analyzer coupled with an isotope ratio mass
258 spectrometer.

259 **2.4 Source apportionment methods**

260 2.4.1 Hydrochemical analysis method

261 (1) Piper diagram

262 The method used to determine the hydrochemical type of groundwater is the
263 Schoeller classification method. First, the concentrations of K^+ , Na^+ , Ca^{2+} , Mg^{2+} , HCO_3^- ,
264 SO_4^{2-} , Cl^- , and NO_3^- -N in groundwater samples, expressed in milligrams per liter (mg
265 L^{-1}), are converted to milliequivalent concentrations (meq L^{-1}). Subsequently, the
266 milliequivalent percentage of each ion is calculated. Finally, the hydrochemical type is
267 determined based on the ions with a milliequivalent percentage greater than 25%. The
268 milliequivalent percentages of cations and anions for all water samples in the water
269 quality monitoring data are plotted on a Piper diagram.

270 (2) PCA-APCS-MLR

271 Principal [Component component Analysis-analysis](#) (PCA) was employed to extract
272 the dominant pollution factors, and the potential sources of groundwater contamination
273 were inferred in conjunction with water quality indicators:

274

$$\left\{ \begin{array}{l} PC_1 = \mu_{11}x_1 + \mu_{12}x_2 + \dots + \mu_{1j}x_j \\ \vdots \\ PC_2 = \mu_{21}x_1 + \mu_{22}x_2 + \dots + \mu_{2j}x_j \\ \vdots \\ PC_m = \mu_{m1}x_1 + \mu_{m2}x_2 + \dots + \mu_{mj}x_j \end{array} \right. \quad (1)$$

275 PC₁, PC₂, ..., PC_m represent the principal components 1, 2, ..., m that can explain the
 276 original indicators. The eigenvalues λ_m ($m \leq j$) of the correlation coefficient matrix are
 277 the variances of PC_m, and the larger the variance, the greater the contribution to the
 278 principal component.

279 Subsequently, on the basis of PCA, the absolute principal component scores (APCS)
 280 were determined. A multiple linear regression (MLR) was performed with the measured
 281 pollutant concentrations as the dependent variables and the absolute principal
 282 component scores as the independent variables (Thurston and Spengler, 1985). The
 283 pollution contributions of each factor were calculated based on the regression
 284 coefficients, thereby determining the contribution rates of the pollution sources;

带格式的: 定义网格后自动调整右缩进, 孤行控制

$$(A_0)_p = \sum_{j=1}^j S_{pj}(Z_0)_j \quad (2)$$

286 p represents the principal component extracted during the principal component analysis
 287 (PCA) process. $(A_0)_p$ denotes the absolute principal component score for principal
 288 component p . S_{pj} represents the scoring coefficient of indicator j within principal
 289 component p .

设置了格式: 字体颜色: 自动设置

$$C_j = b_j + \sum_{p=1}^p b_{pj} \times APCS_{ip} \quad (3)$$

291 C_j represents the measured concentration of pollutant j . b_j denotes the constant term in
 292 the multiple linear regression analysis. b_{pj} represents the regression coefficient for
 293 principal component p . $b_{pj} \times APCS_{ip}$ indicates the concentration contribution of principal
 294 component p to pollutant j in sample i . The average value of $b_{pj} \times APCS_{ip}$ represents the
 295 average concentration contribution of principal component p (the pollution source) to

296 pollutant j . Finally, by converting the concentration contributions of each pollution
297 source into percentages, the contribution rates of the pollution sources can be
298 determined.

299 2.4.2 MixSIAR method

300 The principle of the MixSIAR method is to use the Dirichlet distribution as the prior
301 distribution and to obtain the posterior distribution characteristics of the contributions,
302 such as the mean, variance, and probability density, through the application of Bayes'
303 theorem (Moore and Semmens, 2008). Assuming there are n samples, k different
304 sources, and j isotopes, the MixSIAR mixing model can be expressed as follows:

$$\begin{aligned} 305 \quad X_{ij} &= \sum_{k=1}^K P_k (S_{jk} + \varepsilon_{jk}) + v_{ij} \\ 306 \quad S_{jk} &\sim N(\mu_{jk}, \omega_{jk}^2) \\ 307 \quad \varepsilon_{jk} &\sim N(\lambda_{jk}, \tau_{jk}^2) \\ 308 \quad v_{ij} &\sim N(0, \sigma_j^2) \end{aligned} \quad (4)$$

309 X_{ij} represents the value of the j isotope in the i sample ($i=1, 2, 3, \dots, N$; $j=1, 2, 3, \dots,$
310 J). P_k denotes the contribution rate of the k source ($k=1, 2, 3, \dots, K$), which is predicted
311 using the MixSIAR method. S_{jk} represents the value of the j isotope from the k source,
312 with a mean of μ_{jk} and a variance of ω_{jk}^2 . ε_{jk} represents the enrichment coefficient of the
313 j isotope from the k source, with a mean of λ_{jk} and a variance of τ_{jk}^2 . v_{ij} represents the
314 residual, with a mean of 0 and a variance of σ_j^2 .

315 2.5 Data analysis

316 The stable isotope mixing model used in this study was run in the R package
317 MixSIAR (R version x64 4.3.2). Statistical analysis was performed using SPSS 20
318 software. To evaluate the linear relationships between hydrochemical parameters, the
319 Pearson correlation coefficient (r) was calculated. Correlations were considered
320 statistically significant at a two-tailed p-value < 0.05. The Pearson correlation test was
321 employed to evaluate the relationships between hydrochemical indices, with data

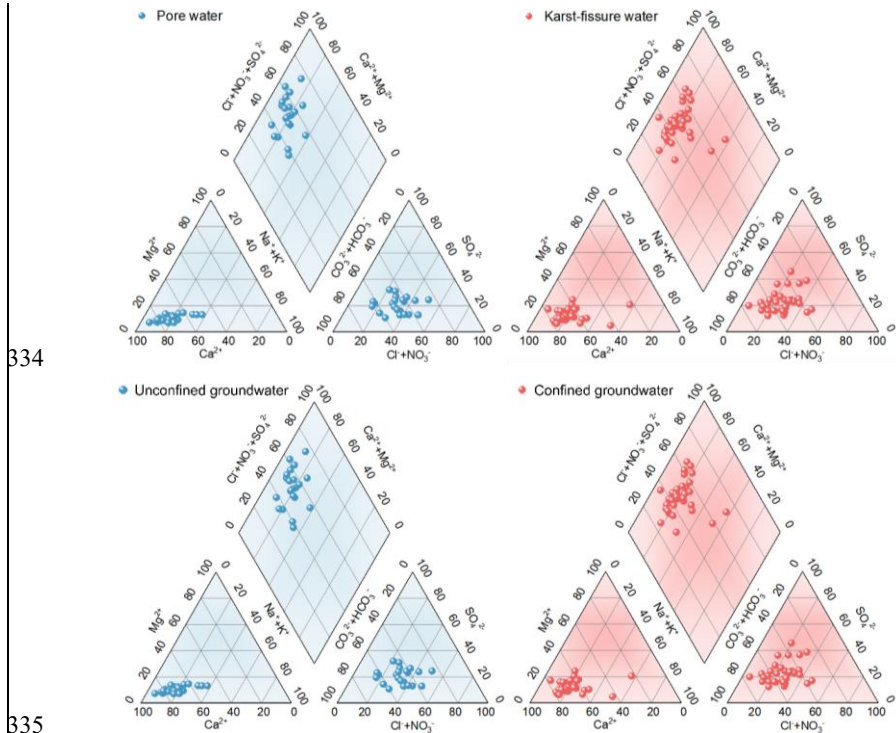
322 analysis conducted using SPSS 20. The spatial distribution of NO_3^- -N concentrations
 323 was generated using Surfer 15 software, and the cartographic work was completed with
 324 Origin 2020.

325

326 3. Results

327 3.1 Characteristics of groundwater NO_3^- -N pollution

328 The type of groundwater in the study area is predominantly of the Ca-type, with the
 329 molar percentage of Ca^{2+} exceeding 50% in most sampling points (Fig.2). In addition,
 330 the groundwater in the study area can be classified into two main types: $\text{Cl}^- \cdot \text{NO}_3^- \cdot \text{HCO}_3^-$
 331 $-\text{Ca}^{2+}$ and $\text{Cl}^- \cdot \text{NO}_3^- \cdot \text{SO}_4^- \cdot \text{Ca}^{2+}$. Specifically, the $\text{Cl}^- \cdot \text{NO}_3^- \cdot \text{HCO}_3^- \cdot \text{Ca}^{2+}$ type is primarily
 332 found in karst water, while the $\text{Cl}^- \cdot \text{NO}_3^- \cdot \text{SO}_4^- \cdot \text{Ca}^{2+}$ type is mainly distributed in pore
 333 water.



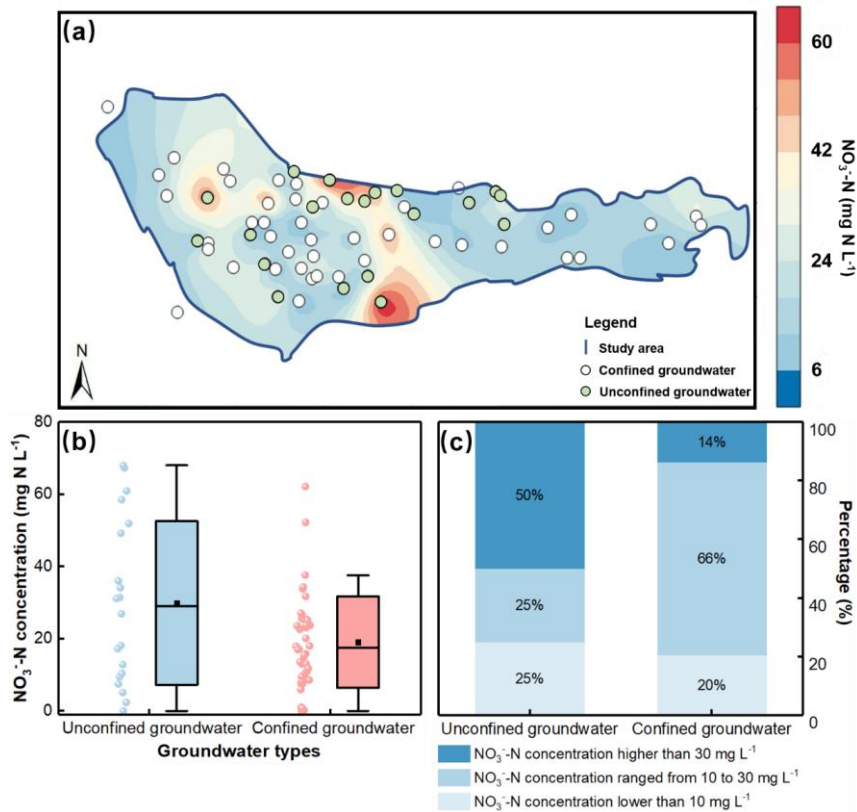
334

335

336 **Fig.2.** Piper graph illustrating hydrochemical types of groundwater.

337 Kriging interpolation was employed to analyze the spatial distribution of NO_3^- -N

338 concentration in the groundwater of the study area. The results indicate that the NO₃⁻-
339 N concentration in the groundwater ranges from 0 to 68 mg N L⁻¹, with an average
340 concentration of 22.45 mg N L⁻¹ (Fig.3). Based on the [standard for drinking water](#)
341 [quality of China](#)~~World Health Organization's drinking water standard~~ (NO₃⁻-N ≤ 10 mg
342 N L⁻¹), the NO₃⁻-N exceedance rate in the study area is 75%, indicating a relatively
343 severe overall pollution status. Specifically, the NO₃⁻-N concentration in unconfined
344 groundwater ranges from 0 to 68 mg N L⁻¹, with an average concentration of 29.9 mg
345 N L⁻¹, while that in confined groundwater ranges from 0 to 62.1 mg N L⁻¹, with an
346 average concentration of 20.1 mg N L⁻¹. Additionally, 50% of the sampling sites in
347 unconfined groundwater and 14% in confined groundwater exceed 30 mg N L⁻¹ (Class
348 V groundwater quality standard ~~in~~^{of} China), suggesting that NO₃⁻-N pollution in
349 unconfined groundwater is more severe than that in confined groundwater. Spatially,
350 the NO₃⁻-N pollution in the groundwater exhibits significant spatial heterogeneity, with
351 the central part of the study area experiencing more severe NO₃⁻-N contamination
352 compared to the western and eastern regions.



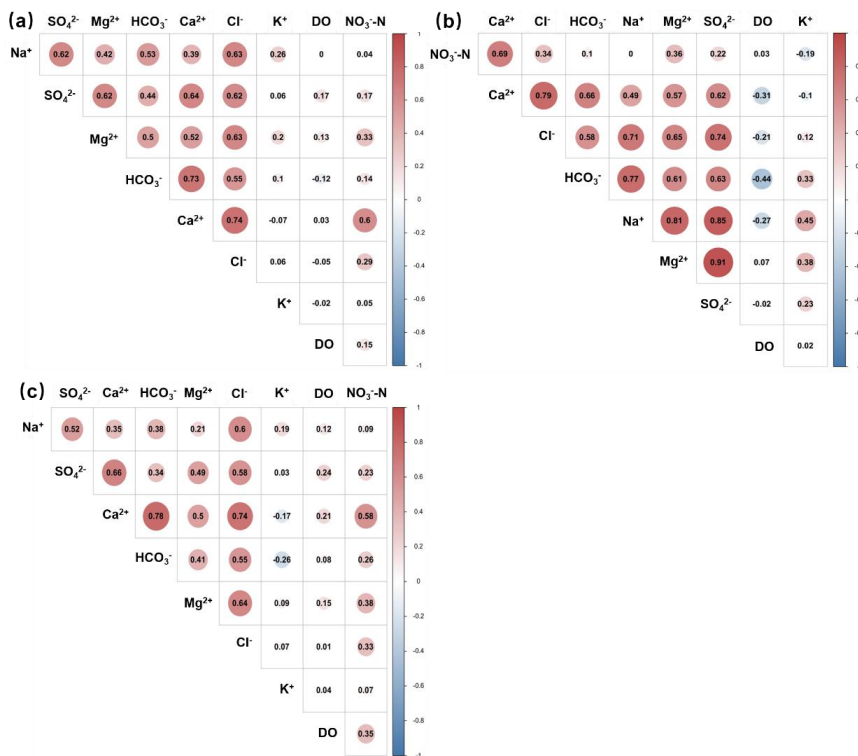
353
 354 **Fig.3.** (a) Spatial distribution map of NO₃-N concentrations in unconfined and confined
 355 groundwater of the study region. (b) Boxplot of NO₃-N concentrations. The dot and line represent
 356 mean value and median. (c) Percentages of NO₃-N concentrations in unconfined groundwater and
 357 confined groundwater (<10 mg N L⁻¹, ranging from 10 to 30 mg N L⁻¹, and >30 mg N L⁻¹).

358 3.2 NO₃-N sources apportionment by PCA-APCS-MLR model

359 3.2.1 Qualitative identification of NO₃-N sources

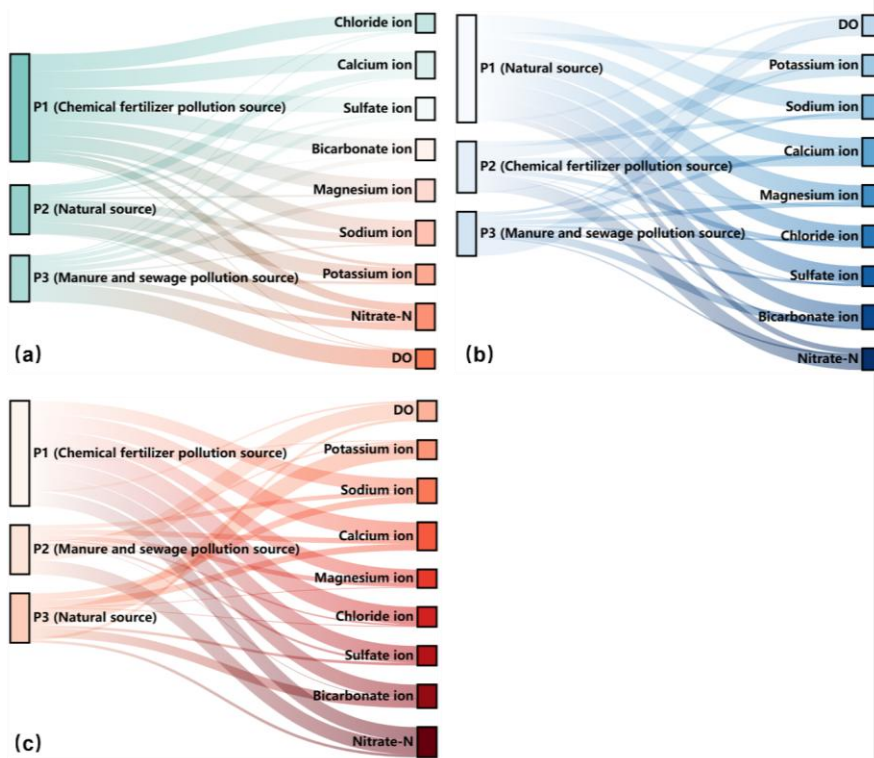
360 The results of Pearson correlation analysis demonstrate that, in the generalized
 361 single-layer aquifer (refers to the simplified analytical scenario in which groundwater
 362 samples from both unconfined and confined aquifers are pooled and treated as a single
 363 homogeneous aquifer, without considering differences in occurrence conditions)
 364 without consideration of aquifer burial conditions (hereinafter referred to as the
 365 generalized single layer aquifer)-(Fig.4a), there is a strong correlation among the nine

366 hydrochemical indicators. For example, Mg^{2+} is strongly correlated with Na^+ , Ca^{2+} , Cl^- ,
 367 SO_4^{2-} , HCO_3^- , and NO_3^- , while NO_3^- exhibits strong correlations with Ca^{2+} , Mg^{2+} , and
 368 Cl^- . In the actual double-layer aquifer (refers to the realistic scenario in which
 369 unconfined and confined aquifers are analyzed separately, respecting their distinct
 370 hydrogeological settings, recharge mechanisms, and pollution pathways) where aquifer
 371 burial conditions are taken into account (hereinafter referred to as the actual double-
 372 layer aquifer) (Fig.4b and Fig.4c), the indicators also show strong correlations.
 373 Specifically, Ca^{2+} is strongly correlated with Na^+ , Mg^{2+} , Cl^- , SO_4^{2-} , HCO_3^- , and NO_3^- ,
 374 and NO_3^- displays strong correlations with DO, Ca^{2+} , Mg^{2+} , and Cl^- . Therefore, the
 375 selected hydrochemical indicators are suitable for principal component analysis.



376
 377 **Fig.4.** Pearson correlation analysis of different hydrochemical indexes. (a) Generalized single-layer
 378 aquifer. (b) Actual double-layer aquifer (unconfined groundwater). (c) Actual double-layer aquifer
 379 (confined groundwater).

380 Subsequently, we calculated the rotated factor loadings using the varimax rotation
 381 method. The factor loadings reflect the relative importance of each variable in the
 382 principal components. Typically, factor loadings greater than 0.7, between 0.7 and 0.5,
 383 and between 0.5 and 0.3 are defined as strong, moderate, and weak loadings,
 384 respectively. Based on these factor loading results, we identified pollution sources. The
 385 results indicate that, for the generalized single-layer aquifer (Fig.5a), P1 represents
 386 pollution from chemical fertilizers, P2 represents natural sources, and P3 represents
 387 pollution from manure & sewage. For the actual double-layer aquifer, in the unconfined
 388 groundwater, P1 represents natural sources, P2 represents pollution from chemical
 389 fertilizers, and P3 represents pollution from manure & sewage. In the confined
 390 groundwater, P1 represents pollution from chemical fertilizers, P2 represents pollution
 391 from manure & domestic sewage, and P3 represents natural sources.



392
 393 **Fig.5.** Sankey graph of rotation factor load matrix for hydrochemical indexes. (a) Generalized

394 single-layer aquifer. (b) Actual double-layer aquifer (unconfined groundwater). (c) Actual double-
 395 layer aquifer (confined groundwater).

396 3.2.2 Quantitative apportionment of NO₃⁻-N sources

397 Following the qualitative identification of the major pollution sources, the APCS-
 398 MLR method was employed to quantitatively analyze the pollution sources (Table 1).

399 For the generalized single-layer aquifer, the regression equation between NO₃⁻-N
 400 concentration and the absolute principal component scores was established as:

401 $C=7.231 \times P1-9.786 \times P2+5.655 \times P3-4.45$ ($R^2=0.789$, $p < 0.01$). This regression model

402 explains 78.9% of the variation in NO₃⁻-N concentration, with the remaining 21.1%

403 attributable to unknown pollution sources. For the actual double-layer aquifer, in the

404 unconfined aquifer, the regression equation between NO₃⁻-N concentration and the

405 absolute principal component scores is: $C=6.85 \times P1+17.84 \times P2+3.78 \times P3+3.197$

406 ($R^2=0.838$, $p < 0.01$), explaining 83.8% of the variation in NO₃⁻-N concentration, and

407 the remaining 16.2% is attributed to unknown pollution sources. In the confined aquifer,

408 the regression equation is: $C=5.12 \times P1+9.16 \times P2-1.74 \times P3-9.26$ ($R^2=0.841$, $p < 0.01$),

409 accounting for 84.1% of the variation in NO₃⁻-N concentration, with the remaining 15.9%

410 attributed to unknown pollution sources.

411 **Table 1.** Multiple regression equation based on APCS-MLR.

Aquifers	Multiple regression equation
Single-layer aquifer	$C=7.231 \times P1-9.786 \times P2+5.655 \times P3-4.45$
Double-layer aquifer (unconfined groundwater)	$C=6.85 \times P1+17.84 \times P2+3.78 \times P3+3.197$
Double-layer aquifer (confined groundwater)	$C=5.12 \times P1+9.16 \times P2-1.74 \times P3-9.26$

412 Furthermore, we calculated the contribution rates of each pollution source using the
 413 regression equations (Fig.6). For the generalized single-layer aquifer, the contribution

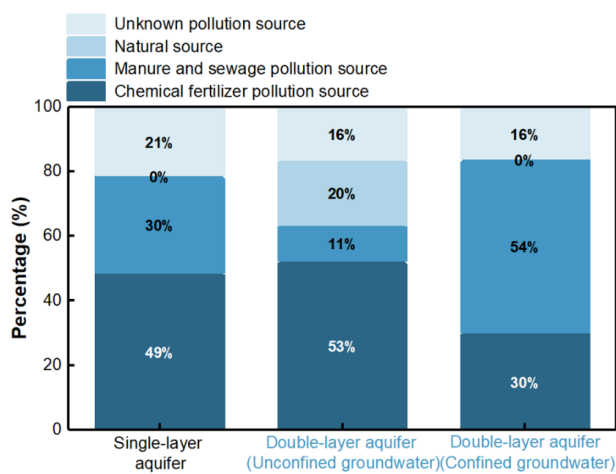
414 rates of chemical fertilizers, manure & sewage, natural sources, and unknown pollution

415 sources were 48.75%, 30.15%, 0%, and 21.1%, respectively, with chemical fertilizers

416 being the dominant pollution source. For the actual double-layer aquifer, in the

417 unconfined groundwater, the contribution rates of chemical fertilizers, manure &

418 sewage, natural sources, and unknown pollution sources were 52.51%, 11.13%, 20.16%,
 419 and 16.2%, respectively. In the confined groundwater, the contribution rates were 30.15%
 420 for chemical fertilizers, 53.95% for manure & sewage, 0% for natural sources, and 15.9%
 421 for unknown pollution sources. Chemical fertilizers and manure & sewage were
 422 identified as the primary pollution sources in the unconfined and confined groundwater,
 423 respectively.



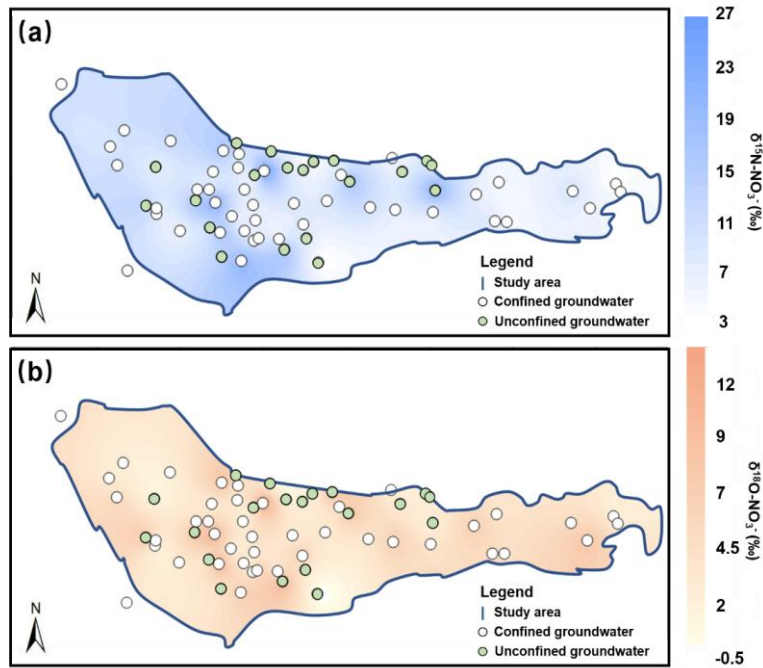
424
 425 **Fig.6.** Quantitative apportionment of NO_3^- -N source based on the PCA-APCS-MLR method

426 **3.3 NO_3^- -N sources apportionment by MixSIAR model**

427 **3.3.1 Distribution characteristics of $\delta^{15}\text{N}$ and $\delta^{18}\text{O}$ in groundwater**

428 We analyzed the $\delta^{15}\text{N}$ and $\delta^{18}\text{O}$ values of NO_3^- -N in potential pollution sources
 429 (atmospheric deposition, soil nitrogen, chemical fertilizers, and manure & sewage) as
 430 well as in groundwater within the study area. The results of the $\delta^{15}\text{N}$ and $\delta^{18}\text{O}$ values
 431 for the potential pollution sources are presented in the Supplementary data (S1). The
 432 $\delta^{15}\text{N}$ and $\delta^{18}\text{O}$ values of NO_3^- -N in groundwater within the study area are shown in
 433 Fig.7. For the generalized single-layer aquifer, the $\delta^{15}\text{N}$ values range from 2.8‰ to
 434 29.29‰, with an average of 9.85‰, while the $\delta^{18}\text{O}$ values range from -0.85‰ to
 435 15.12‰, with an average of 4.42‰. For the actual double-layer aquifer, the average
 436 $\delta^{15}\text{N}$ and $\delta^{18}\text{O}$ values in unconfined groundwater are 10.16‰ and 3.93‰, respectively,
 437 and in confined groundwater, the average $\delta^{15}\text{N}$ and $\delta^{18}\text{O}$ values are 9.71‰ and 4.6‰,

438 respectively.



439

440 **Fig.7.** Spatial distribution of $\delta^{15}\text{N-NO}_3^-$ (a) and $\delta^{18}\text{O-NO}_3^-$ (b) in the groundwater

441 3.3.2 Qualitative identification of NO_3^- -N sources

442 The NO_3^- -N in the groundwater of the study area originates from multiple nitrogen
443 pollution sources. Given the distinct isotopic signatures of $\delta^{15}\text{N}$ and $\delta^{18}\text{O}$ of NO_3^- -N
444 from different sources, qualitative identification of groundwater NO_3^- -N sources can be
445 achieved based on the characteristic ranges of these dual isotopes. As shown in Fig.8,
446 the majority of the $\delta^{15}\text{N}$ and $\delta^{18}\text{O}$ values in groundwater locate within the [ranges](#)
447 characteristic [ranges](#) of chemical fertilizers, soil nitrogen, and manure & sewage. This
448 indicates that the NO_3^- -N in the groundwater of the study area is primarily derived from
449 these three pollution sources.

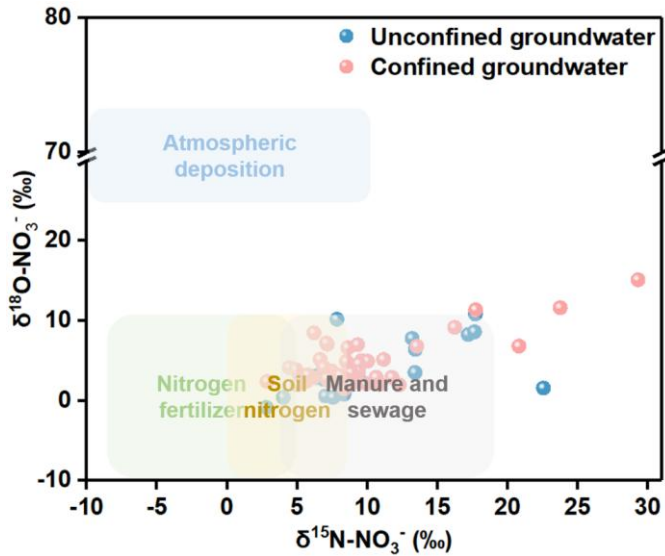
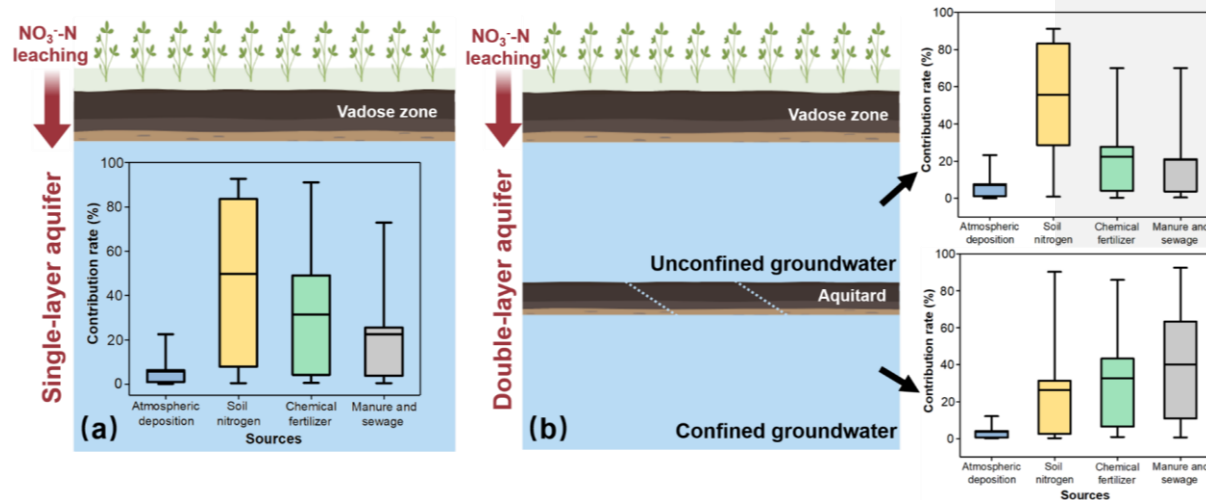


Fig.8. Isotopic ratio plot of $\delta^{15}\text{N}$ and $\delta^{18}\text{O}$ of NO_3^- -N in Groundwater

3.3.3 Quantitative apportionment of NO_3^- -N sources

The $\delta^{15}\text{N}$ and $\delta^{18}\text{O}$ values of groundwater samples, as well as the mean values and standard deviations of $\delta^{15}\text{N}$ and $\delta^{18}\text{O}$ for potential pollution sources, were used as known parameters and input into the MixSIAR method. To account for potential errors caused by isotopic fractionation, we calculated the fractionation coefficients for $\delta^{15}\text{N}$ and $\delta^{18}\text{O}$ of different pollution sources (Supplementary data, S2) and incorporated these coefficients into the MixSIAR method. Ultimately, by treating the contribution rates of different pollution sources as random variables, we established probabilistic distribution equations for pollution source contributions using the MixSIAR method, thereby determining the extent to which each pollution source contributes to NO_3^- -N pollution in groundwater. The results indicate that, for the generalized single-layer aquifer (Fig.9a), the contribution rates of atmospheric deposition, soil nitrogen, chemical fertilizers, and manure & sewage to NO_3^- -N pollution are 4.6%, 49.5%, 27.8%, and 18.1%, respectively. For the actual double-layer aquifer (Fig.9b), in the unconfined groundwater, the contribution rates of atmospheric deposition, soil nitrogen, chemical fertilizers, and manure & sewage to NO_3^- -N pollution are 5.7%, 58%, 20.1%, and

468 16.2%, respectively. In the confined groundwater, the contribution rates of these four
 469 pollution sources are 3.1%, 27.5%, 31.5%, and 37.9%, respectively.



470 **Fig.9.** Quantitative apportionment of NO₃-N source based on the MixSIAR method. (a)
 471 Generalized single-layer aquifer. (b) Actual double-layer aquifer.

472

473 4. Discussion

474 We employed both the PCA-APCS-MLR method and the MixSIAR method to
 475 quantitatively identify the sources of NO₃-N in aquifers/groundwater under different
 476 burial/occurrence conditions. For the PCA-APCS-MLR analysis, different ions exhibit
 477 varying loading strengths in each principal component. Therefore, through
 478 hydrochemical analysis and statistical methods, we can calculate and infer the type of
 479 pollution source represented by each principal component. For example, in unconfined
 480 groundwater, Na⁺, Ca²⁺, Mg²⁺, HCO₃⁻, SO₄²⁻, and Cl⁻ have strong loadings in P1. These
 481 ions are all major ions in groundwater, and their average concentrations are relatively
 482 low. Moreover, correlation analysis results show that the concentration of NO₃⁻-N has
 483 very low correlation with the concentrations of Na⁺, Mg²⁺, HCO₃⁻, SO₄²⁻, and Cl⁻,
 484 indicating that NO₃⁻-N does not originate from the same source as these ions (Yu et al.,
 485 2022). Thus, it is demonstrated that P1 represents a natural source. In P2, Ca²⁺ and NO₃⁻

486 -N have strong loadings. The correlation results (Fig.4) indicate a significant positive
487 correlation ($p < 0.01$) between Ca^{2+} and NO_3^- -N, suggesting that Ca^{2+} originates from
488 anthropogenic pollution. ~~This is because~~ Ca^{2+} ~~calcium~~ is required in the cultivation of
489 tomatoes and cucumbers (the main crop types in the study area), and the extensive use
490 of calcium fertilizers during the application of base fertilizers and top-dressing
491 fertilizers also increases the concentration of Ca^{2+} in groundwater (Schot and Wassen,
492 1993). Therefore, P2 primarily represents the pollution source from chemical fertilizers.
493 In P3, DO has a strong loading. Since the oxidation and decomposition of organic
494 matter require a large amount of DO (Díaz-Cruz and Barceló, 2008), the strong loading
495 of DO is associated with organic pollution of groundwater (such as from manure ~~&and~~
496 ~~domestic~~ sewage). Thus, P3 mainly represents the pollution sources of manure &
497 sewage. After determining the pollution sources represented by each principal
498 component using the above methods, we can calculate the contribution rate of each
499 pollution source using regression equations. The PCA-APCS-MLR method has the
500 advantages of being rapid and convenient, but it has the disadvantage of being unable
501 to further identify soil nitrogen as a pollution source. Accurately apportioning soil-
502 derived NO_3^- -N is particularly challenging for hydrochemical-based methods due to the
503 overlapping ionic signatures between soil nitrogen and the leaching of synthetic
504 fertilizers or organic wastes (Yu et al., 2022). To compensate for this limitation, the
505 MixSIAR method was further employed to analyze the sources of pollution. We
506 identified soil nitrogen as another important source of NO_3^- -N in groundwater.
507 Additionally, we incorporated isotope fractionation coefficients into the
508 ~~calculations~~ MixSIAR model. ~~This is because~~ NO_3^- -N from different sources
509 (atmospheric deposition, soil nitrogen, chemical fertilizers, and manure & sewage) has
510 distinct isotopic signatures, and isotopic fractionation occurs during the transport and
511 transformation processes of nitrogen in the groundwater system (such as
512 ammonification and nitrification), leading to changes in the $\delta^{15}\text{N}$ and $\delta^{18}\text{O}$ values of
513 NO_3^- -N (Shu et al., 2024). Our MixSIAR model incorporated fractionation factors of

514 specific nitrogen transformation processes. This approach, essential for reliable
515 quantification, aligns with established practice in NO₃⁻-N source apportionment studies,
516 where such constraints are proven to substantially reduce uncertainty. Therefore,
517 considering the effect of isotope fractionation can better eliminate uncertainties in
518 nitrogen transformation processes and significantly improve the accuracy of source
519 apportionment results. This approach has also been confirmed by previous studies
520 (Wang et al., 2023; Yu et al., 2020).

521 In this study, the PCA-APCS-MLR method identified chemical fertilizers as the
522 primary source of NO₃⁻-N in unconfined groundwater and manure & sewage as the
523 main sources of NO₃⁻-N in confined groundwater. The MixSIAR method further
524 revealed that soil nitrogen is a dominant pollution source for unconfined groundwater,
525 with a higher contribution rate than that of chemical fertilizers. The identification of
526 soil nitrogen as a major contributor in the unconfined groundwater is significant.
527 Legacy soil nitrogen constitutes a dominant source in the unconfined groundwater, a
528 finding that shifts the pollution focus from direct fertilizer inputs to cumulative soil
529 nitrogen pools. This result is consistent with previous NO₃⁻-N source studies conducted
530 in other regions (Cui et al., 2023). ~~For confined groundwater, MixSIAR also confirmed~~
531 ~~that manure & sewage are the major sources of NO₃⁻-N.~~ The findings for unconfined
532 groundwater can be attributed to the extensive use of chemical fertilizers in agricultural
533 production (Hao et al., 2025). Nitrogen from these fertilizers can directly leach into the
534 unconfined ~~aquifer~~groundwater, causing NO₃⁻-N pollution (Xie et al., 2025).
535 Additionally, excess nitrogen accumulates in the soil and vadose zone, where it is
536 transformed from organic nitrogen to NH₄⁺-N and then to NO₃⁻-N under the action of
537 soil microorganisms (Liu et al., 2023). While NH₄⁺-N can be adsorbed and immobilized
538 by the soil, NO₃⁻-N can leach into the deeper vadose zone and aquifer through
539 atmospheric precipitation or agricultural irrigation, directly contaminating unconfined
540 groundwater (Wan et al., 2024). This process underscores the phenomenon of the soil
541 and vadose zone as a dynamic “nitrogen reactor and buffer”. Similar delayed release

设置了格式: 字体颜色: 深红

设置了格式: 字体颜色: 深红

542 [mechanisms from legacy nitrogen stored in thick unsaturated zones have been](#)
543 [documented in arid regions \(Li et al., 2025\), indicating that the risk of groundwater](#)
544 [contamination may persist long after surface inputs are reduced.](#) Therefore, in assessing
545 the sources of NO₃⁻-N pollution in regional groundwater, it is crucial not only to focus
546 on the application rates of chemical fertilizers but also to pay attention to the storage of
547 nitrogen in the soil and vadose zone. These accumulated nitrogen compounds can
548 continuously leach into unconfined groundwater under external disturbances (such as
549 irrigation or precipitation), leading to persistent contamination (Niu et al., 2022).
550 Therefore, it is essential to guide local farmers in implementing surface management
551 practices (such as the use of chemical fertilizers and the application of manure) to
552 enforce optimal agricultural irrigation policies, including reducing irrigation frequency,
553 to delay the transport of stored nitrogen in ~~the~~ soil to ~~the aquifer~~ groundwater. [For](#)
554 [confined groundwater, the MixSIAR method also confirmed that manure & sewage](#)
555 [are the major sources of NO₃⁻-N. Regarding the results for confined](#)
556 [groundwater](#) Generally, the nitrogen in manure ~~&~~ sewage primarily exists in the form
557 of large molecules. These complex nitrogen compounds are difficult to degrade
558 microbially or transform chemically in a short period, leading to their long-term
559 persistence in the environment. These pollutants can enter surface water bodies through
560 surface runoff or infiltration and then gradually transport to deeper aquifers via the
561 interflow recharge process between unconfined and confined aquifers, resulting in
562 persistent contamination (McDonough et al., 2022). [This may highlight a potential](#)
563 [mechanism for sustained NO₃⁻-N pollution in confined systems, which can be attributed](#)
564 [to manure & sewage sources transported via aquifer exchange, providing a continuous](#)
565 [input of recalcitrant nitrogen that gradually accumulates in this zone \(Zhang et al.,](#)
566 [2026\).](#) Therefore, for the prevention and control of NO₃⁻-N pollution in confined
567 [aquifers](#) groundwater, it is crucial to focus on the source control of manure & sewage to
568 block the migration pathways of pollutants and mitigate their long-term impacts ~~on~~
569 [confined aquifers.](#)

570 ~~This study compared the errors in source apportionment of NO₃⁻-N in aquifers with and~~
571 ~~without consideration of burial conditions. The absolute errors for the PCA-APCS-~~
572 ~~MLR method were 4%–20% and 5%–24%, while those for the MixSIAR method were~~
573 ~~1.1%–8.5% and 1.5%–22%. The causes of these errors can be attributed to two main~~
574 ~~factors.~~

575 This study assessed the discrepancy in source apportionment of NO₃⁻-N in
576 groundwater obtained under different groundwater occurrence conditions. This
577 discrepancy can be attributed to two main factors. First, the sources and recharge
578 mechanisms of groundwater in unconfined and confined aquifers differ significantly
579 ([Liu et al., 2025](#)), leading to distinct isotopic compositions and characteristic values.
580 For example, the isotopic signature of a pollution source in an unconfined aquifer may
581 resemble that of another source in a confined aquifer. [Such overlapping isotopic signals](#)
582 [can lead to ambiguous source identification. However, previous studies either do not](#)
583 [explicitly distinguish between groundwater occurrence conditions or rely on land-use](#)
584 [as a primary proxy for pollution source identification \(Yu et al., 2020\).](#) When mixed
585 calculations are performed without considering the actual ~~burial~~occurrence conditions,
586 the isotopic differences are obscured, ~~resulting in confusion in pollution source~~
587 ~~identification, inaccurate contribution rate calculations, and incomplete analysis of~~
588 ~~pollution processes. This, in turn, which~~ may lead to an underestimation or
589 overestimation of the pollution source contributions ~~of pollution sources~~ to
590 groundwater ~~under different burial~~occurrence conditions. Second, the migration and
591 transformation capacities of nitrogen vary among different geological strata.
592 Hydrogeological conditions can influence the intensity of biogeochemical processes
593 such as ammonification, nitrification, denitrification ([Dai et al., 2023](#)), and adsorption
594 (Huang et al., 2022; Li et al., 2023), which further alter NO₃⁻-N concentrations and
595 isotopic signatures. This ultimately affects the accuracy and reliability of pollution
596 source apportionment. Consequently, effective nitrate management of NO₃⁻-N in
597 groundwater systems requires policy interventions tailored to specific aquifer

带格式的: 定义网格后自动调整右缩进, 孤行控制

598 ~~burial~~groundwater occurrence conditions. In unconfined ~~aquifers~~groundwater, which
599 are highly vulnerable to surface-derived inputs, management should prioritize
600 agricultural best practices such as optimized irrigation scheduling — reducing both
601 frequency and volume of irrigation — coupled with the promotion of slow-release or
602 stabilized nitrogen fertilizers. These measures can significantly decrease the rapid
603 leaching of soil nitrogen pools, thereby mitigating short-term, ~~large-scale pulses of~~
604 ~~NO₃⁻-N~~ into groundwater. ~~nitrate spikes~~. Additionally, ~~land use zoning that limits~~
605 ~~intense agricultural or livestock activities near recharge areas could further reduce~~
606 ~~nitrate loading~~. In contrast, ~~e~~Besides, the confined ~~aquifers~~groundwater, often affected
607 by legacy pollution, requires long-term strategies focused on source control. This
608 includes stricter regulation and monitoring of manure storage facilities, improved
609 wastewater treatment infrastructure, and the implementation of containment systems to
610 prevent leaching from historical contamination hotspots. Given the limited attenuation
611 capacity and persistent nature of NO₃⁻-N in confined ~~aquifers~~groundwater, remediation
612 efforts may also need to consider engineered attenuation or pump-and-treat systems in
613 severely affected zones. Future research should integrate reactive-transport modeling
614 with isotopic mixing models to better capture the dynamic behavior of nitrogen in
615 dual-layer aquifer systems and to further reduce uncertainty in source apportionment
616 under varying hydrogeological conditions. ~~pollution control measures may deviate from~~
617 ~~actual needs and fail to effectively mitigate and reduce NO₃⁻-N contamination in~~
618 ~~groundwater.~~

设置了格式: 字体: 非加粗

设置了格式: 字体: 非加粗

设置了格式: 字体: (默认) Times New Roman, 字体颜色: 自动设置, 图案: 清除

设置了格式: 字体颜色: 深红

619

620 5. Conclusion

621 The study ~~quantitatively investigated~~ analyzed the ~~pollution~~ sources of NO₃⁻-N
622 ~~pollution~~ in ~~aquifers~~groundwater under different ~~burial~~occurrence conditions ~~using~~
623 ~~PCA-APCS-MLR and MixSIAR methods.~~ ~~and analyzed the errors in source~~
624 ~~apportionment results of NO₃⁻-N pollution in groundwater when ~~burial~~occurrence~~
625 ~~conditions were not considered~~. The results showed that the groundwater NO₃⁻-N

626 concentration in the study area ranged from 0 to 68 mg N L⁻¹, with an exceedance rate
627 of 75%. The NO₃⁻-N pollution in unconfined groundwater (average concentration 29.9
628 mg N L⁻¹) was more severe than that in confined groundwater (average concentration
629 20.1 mg N L⁻¹). NO₃⁻-N in unconfined groundwater predominantly originates from soil
630 nitrogen (58%), with a non-negligible contribution from chemical fertilizers. Therefore,
631 it is necessary to focus on the storage of nitrogen in the soil and improve agricultural
632 irrigation practices to prevent rapid infiltration of NO₃⁻-N into unconfined groundwater,
633 which could lead to persistent contamination. NO₃⁻-N enrichment in confined
634 groundwater is primarily attributed to manure & sewage (37.9%).~~The PCA-APCS-~~
635 ~~MLR method confirmed that the chemical fertilizer is the primary source of NO₃⁻-N in~~
636 ~~unconfined groundwater, while the MixSIAR method further identified soil nitrogen as~~
637 ~~the main source of NO₃⁻-N pollution in unconfined groundwater, with a higher~~
638 ~~contribution rate than that of chemical fertilizers. Therefore, it is necessary to focus on~~
639 ~~the storage of nitrogen in the soil and improve agricultural irrigation practices to prevent~~
640 ~~rapid infiltration of NO₃⁻-N into unconfined groundwater, which could lead to persistent~~
641 ~~contamination. For the confined groundwater, manure & sewage constitute the~~
642 dominant sources of NO₃⁻-N. Regulations and infrastructure for the treatment and
643 disposal of domestic sewage and livestock waste should be strengthened to prevent their
644 extensive accumulation ~~in infiltration into the~~ confined groundwater. Ignoring the
645 groundwater occurrence conditions leads to marked deviations in the source
646 apportionment results. ~~Therefore, pollution source identification and control policies~~
647 ~~for groundwater groundwater risk assessments and pollution control strategies must~~
648 explicitly distinguish between unconfined and confined groundwater. Management
649 policies and monitoring programs should be tailored to the specific dominant sources
650 and vulnerability of each aquifer type. Both analytical methods indicated that manure
651 & sewage are the main sources of NO₃⁻-N in confined groundwater. When the
652 burial occurrence conditions of groundwater were not considered, both methods yielded
653 significant errors (with absolute errors reaching up to 24%). Thus, to accurately identify

设置了格式: 字体: 非加粗

654 ~~and effectively manage the sources of NO₃⁻-N pollution in groundwater, it is essential~~
655 ~~to carefully incorporate the actual burial occurrence conditions of regional~~
656 ~~aquifers groundwater into the analysis.~~

657

658 **Acknowledgments**

659 This work was supported by [the National Key Research and Development Program](#)
660 [of China \(No. 2024YFC3213900\)](#), the National Natural Science Foundation of China
661 (No. 42422207 [and No. 42507105](#)), [and the Postdoctoral Research Project \(No.](#)
662 [QDBSH20240202055](#)).

663

664 **CRedit authorship contribution statement**

665 **Y L:** Writing – review & editing, Writing – original draft, Visualization, Methodology,
666 Investigation, Formal analysis, Data curation, Conceptualization.

667 **J L:** Writing – review & editing, Supervision, Methodology, Conceptualization.

668 **Y J W:** Writing – review & editing, Supervision, Methodology, Conceptualization.

669 **Z Y Z:** Visualization, Investigation, Methodology, Conceptualization.

670 **X L Z:** Supervision, Conceptualization.

671 **T Y Z:** Writing – review & editing, Supervision, Resources, Methodology, Investigation,
672 Conceptualization, Funding acquisition.

673

674 **Declaration of competing interest**

675 The authors declare that they have no known competing financial interests or
676 personal relationships that could have appeared to influence the work reported in this
677 paper.

678

679 **Data availability statement**

680 The data of this study can be found in Liu (2025), “Data Availability for HESS”,
681 Mendeley Data, V1, doi: 10.17632/53d3ktbg8d.1.

设置了格式: 字体: 非加粗

设置了格式: 非突出显示

682

683 **References**

684 [Cui, R., Zhang, D., Hu, W., Zhao, X., Yan, H., Liu, G., Chen, A., 2023. Nitrogen in soil, manure and](#)
685 [sewage has become a major challenge in controlling nitrate pollution in groundwater around plateau](#)
686 [lakes, Southwest China. J. Hydrol. 620, 129541.](#)

687 [Dai, H., Zhang, Y., Fang, W., Liu, J., Hong, J., Zou, C., Zhang, J., 2023. Microbial community structural](#)
688 [response to variations in physicochemical features of different aquifers. Front. Microbiol. 14,](#)
689 [1025964.](#)

690 Diaz-Cruz, M.S., Barceló, D., 2008. Trace organic chemicals contamination in ground water recharge.
691 Chemosphere 72(3), 333-342.

692 Gibrilla, A., Fianko, J.R., Ganyaglo, S., Adomako, D., Anornu, G., Zakaria, N., 2020. Nitrate
693 contamination and source apportionment in surface and groundwater in Ghana using dual isotopes
694 (^{15}N and ^{18}O - NO_3) and a Bayesian isotope mixing model. J. Contam. Hydrol. 233, 103658.

695 [Greenberg, A.E., Trussell, R.R., Clesceri, L.S., Association, A.W.W., 2005. Standard methods for the](#)
696 [examination of water and wastewater : supplement to the sixteenth edition. American Journal of](#)
697 [Public Health & the Nations Health 56\(3\), 387.](#)

698 Gutiérrez, M., Biagioni, R.N., Alarcón-Herrera, M.T., Rivas-Lucero, B.A., 2018. An overview of nitrate
699 sources and operating processes in arid and semiarid aquifer systems. Sci. Total Environ. 624, 1513-
700 1522.

701 Hao, Y., Zheng, T., Liu, L., Li, P., Ma, H., Zheng, Z., Zheng, X., Luo, J., 2025. Occurrence of
702 dissimilatory nitrate reduction to ammonium (DNRA) in groundwater table fluctuation zones during
703 dissolved organic nitrogen leaching through unsaturated zone. J. Hazard. Mater. 489, 137501.

704 Huang, X., Jin, M., Ma, B., Liang, X., Cao, M., Zhang, J., Zhang, Z., Su, J., 2022. Identifying nitrate
705 sources and transformation in groundwater in a large subtropical basin under a framework of
706 groundwater flow systems. J. Hydrol. 610, 127943.

707 Ji, X., Shu, L., Chen, W., Chen, Z., Shang, X., Yang, Y., Dahlgren, R.A., Zhang, M., 2022. Nitrate
708 pollution source apportionment, uncertainty and sensitivity analysis across a rural-urban river
709 network based on $\delta^{15}\text{N}/\delta^{18}\text{O}$ - NO_3^- isotopes and SIAR modeling. J. Hazard. Mater. 438, 129480.

设置了格式: 字体颜色: 黑色

带格式的: 缩进: 左侧: 0 厘米, 悬挂缩进: 3.2 字符, 行距: 1.5 倍行距

710 Kellman, L.M., Hillaire-Marcel, C., 2003. Evaluation of nitrogen isotopes as indicators of nitrate
711 contamination sources in an agricultural watershed. *Agriculture, ecosystems & environment* 95(1),
712 87-102.

713 Li, J., Liu, Y., Dai, W., Li, J., Yang, P., Tian, L., Yu, S., Zuo, R., Zhai, Y., Song, W., 2023. Nitrate
714 attenuation with rising groundwater levels: An integrated assessment using isotope tracers and
715 microbial signatures. *J. Hydrol.* 624, 129911.

716 [Li, S., Chow, R., Su, H., Han, F., Li, Z., 2025. Multiple isotopes and GIS analyses reveal sources and
717 drivers of nitrate in the Loess Plateau's groundwater. *Environ. Pollut.*, 127022.](#)

718 [Liang, X., Zhan, H., Zhang, Y.K., Schilling, K., 2017. Base flow recession from unsaturated - saturated
719 porous media considering lateral unsaturated discharge and aquifer compressibility. *Water Resour.
720 Res.* 53\(9\), 7832-7852.](#)

721 Liu, S., Zheng, T., Li, Y., Zheng, X., 2023. A critical review of the central role of microbial regulation
722 in the nitrogen biogeochemical process: New insights for controlling groundwater nitrogen
723 contamination. *J. Environ. Manage.* 328, 116959.

724 [Liu, W., Du, Y., Qiu, W., Deng, Y., Wang, Y., 2025. Constraints on vertical variability of geogenic
725 ammonium in multi-layered aquifer systems. *Water Res.* 268, 122639.](#)

726 Liu, Y., Xin, J., Wang, Y., Yang, Z., Liu, S., Zheng, X., 2022. Dual roles of dissolved organic nitrogen
727 in groundwater nitrogen cycling: nitrate precursor and denitrification promoter. *Sci. Total Environ.*
728 811, 151375.

729 Ma, J., Liu, H., Tong, L., Wang, Y., Chen, R., Liu, S., Zhao, L., Li, Z., Cai, L., 2019. Relationships
730 between microbial communities and groundwater chemistry in two pristine confined groundwater
731 aquifers in central China. *Hydrol. Process.* 33(14), 1993-2005.

732 Mao, H., Wang, G., Liao, F., Shi, Z., Zhang, H., Chen, X., Qiao, Z., Li, B., Bai, Y., 2023. Spatial
733 variability of source contributions to nitrate in regional groundwater based on the positive matrix
734 factorization and Bayesian model. *J. Hazard. Mater.* 445, 130569.

735 McDonough, L.K., Andersen, M.S., Behnke, M.I., Rutledge, H., Oudone, P., Meredith, K., O Carroll,
736 D.M., Santos, I.R., Marjo, C.E., Spencer, R.G., 2022. A new conceptual framework for the
737 transformation of groundwater dissolved organic matter. *Nat. Commun.* 13(1), 2153.

设置了格式: 字体: 小四, 字体颜色: 自动设置

设置了格式: 字体: 10 磅

设置了格式: 字体颜色: 深红

738 Meng, L., Zuo, R., Wang, J., Yang, J., Teng, Y., Shi, R., Zhai, Y., 2018. Apportionment and evolution
739 of pollution sources in a typical riverside groundwater resource area using PCA-APCS-MLR model.
740 J. Contam. Hydrol. 218, 70-83.

741 Minet, E.P., Goodhue, R., Meier-Augenstein, W., Kalin, R.M., Fenton, O., Richards, K.G., Coxon, C.E.,
742 2017. Combining stable isotopes with contamination indicators: a method for improved investigation
743 of nitrate sources and dynamics in aquifers with mixed nitrogen inputs. Water Res. 124, 85-96.

744 Moore, J.W., Semmens, B.X., 2008. Incorporating uncertainty and prior information into stable isotope
745 mixing models. Ecol. Lett. 11(5), 470-480.

746 Niu, X., Jia, X., Yang, X., Wang, J., Wei, X., Wu, L., Shao, M., 2022. Tracing the sources and fate of
747 NO₃-in the vadose zone-groundwater system of a thousand-year-cultivated region. Environ. Sci.
748 Technol. 56(13), 9335-9345.

749 Picetti, R., Deeney, M., Pastorino, S., Miller, M.R., Shah, A., Leon, D.A., Dangour, A.D., Green, R.,
750 2022. Nitrate and nitrite contamination in drinking water and cancer risk: A systematic review with
751 meta-analysis. Environ. Res. 210, 112988.

752 Ransom, K.M., Grote, M.N., Deinhart, A., Eppich, G., Kendall, C., Sanborn, M.E., Souders, A.K.,
753 Wimpenny, J., Yin, Q.Z., Young, M., 2016. Bayesian nitrate source apportionment to individual
754 groundwater wells in the Central Valley by use of elemental and isotopic tracers. Water Resour. Res.
755 52(7), 5577-5597.

756 Rivett, M.O., Buss, S.R., Morgan, P., Smith, J.W., Bemment, C.D., 2008. Nitrate attenuation in
757 groundwater: a review of biogeochemical controlling processes. Water Res. 42(16), 4215-4232.

758 Romanelli, A., Soto, D.X., Matiatos, I., Martínez, D.E., Esquius, S., 2020. A biological and nitrate
759 isotopic assessment framework to understand eutrophication in aquatic ecosystems. Sci. Total
760 Environ. 715, 136909.

761 Ruan, D., Bian, J., Wang, Y., Wu, J., Gu, Z., 2024. Identification of groundwater pollution sources and
762 health risk assessment in the Songnen Plain based on PCA-APCS-MLR and trapezoidal fuzzy
763 number-Monte Carlo stochastic simulation model. J. Hydrol. 632, 130897.

764 Schot, P.P., Wassen, M.J., 1993. Calcium concentrations in wetland groundwater in relation to water
765 sources and soil conditions in the recharge area. J. Hydrol. 141(1-4), 197-217.

设置了格式: 字体: 10 磅, 字体颜色: 黑色

766 Shu, L., Chen, W., Liu, Y., Shang, X., Yang, Y., Dahlgren, R.A., Chen, Z., Zhang, M., Ji, X., 2024.
767 Riverine nitrate source identification combining $\delta^{15}\text{N}/\delta^{18}\text{O}-\text{NO}_3^-$ with $\Delta^{17}\text{O}-\text{NO}_3^-$ and a
768 nitrification ^{15}N -enrichment factor in a drinking water source region. *Sci. Total Environ.* 918,
769 170617.

770 [Thurston, G.D., Spengler, J.D., 1985. A quantitative assessment of source contributions to inhalable
771 particulate matter pollution in metropolitan Boston. *Atmospheric Environment \(1967\)* 19\(1\), 9-25.](#)

772 Wan, Y., Li, R., Yao, K., Peng, C., Wang, W., Li, N., Wang, X., 2024. Bioelectro-barriers prevent nitrate
773 leaching into groundwater via nitrogen retention. *Water Res.* 249, 120988.

774 [Wang, D., Li, P., Yang, N., Yang, C., Zhou, Y., Li, J., 2023. Distribution, sources and main controlling
775 factors of nitrate in a typical intensive agricultural region, northwestern China: vertical profile
776 perspectives. *Environ. Res.* 237, 116911.](#)

777 Wong, W.W., Grace, M.R., Cartwright, I., Cook, P.L., 2015. Unravelling the origin and fate of nitrate in
778 an agricultural–urban coastal aquifer. *Biogeochemistry* 122, 343-360.

779 [Xie, L., Li, P., Fida, M., Elumalai, V., 2025. Characteristics and potential health risk of inorganic nitrogen
780 in phreatic water in the central and southern parts of Yinchuan Plain \(Northwest China\). *Expo. Health*
781 17\(2\), 581-598.](#)

782 Xin, J., Liu, Y., Chen, F., Duan, Y., Wei, G., Zheng, X., Li, M., 2019. The missing nitrogen pieces: A
783 critical review on the distribution, transformation, and budget of nitrogen in the vadose zone-
784 groundwater system. *Water Res.* 165, 114977.

785 Xin, J., Wang, Y., Shen, Z., Liu, Y., Wang, H., Zheng, X., 2021. Critical review of measures and decision
786 support tools for groundwater nitrate management: A surface-to-groundwater profile perspective. *J.*
787 *Hydrol.* 598, 126386.

788 Yang, L., Han, J., Xue, J., Zeng, L., Shi, J., Wu, L., Jiang, Y., 2013. Nitrate source apportionment in a
789 subtropical watershed using Bayesian model. *Sci. Total Environ.* 463, 340-347.

790 Yu, L., Zheng, T., Yuan, R., Zheng, X., 2022. APCS-MLR model: a convenient and fast method for
791 quantitative identification of nitrate pollution sources in groundwater. *J. Environ. Manage.* 314,
792 115101.

793 Yu, L., Zheng, T., Zheng, X., Hao, Y., Yuan, R., 2020. Nitrate source apportionment in groundwater

设置了格式: 字体: 10 磅, 字体颜色: 文字 1

设置了格式: 字体: 10 磅

设置了格式: 字体颜色: 深红

794 using Bayesian isotope mixing model based on nitrogen isotope fractionation. Sci. Total Environ.
795 718, 137242.

796 [Zhang, T., Lei, Q., Liu, H., Ding, K., Luo, J., Qiu, W., Ma, Y., Xu, Q., Zhao, Y., Liu, X., 2026. Vertical](#)
797 [migration of multi-source nitrates driven by multiple water inputs in groundwater base on combined](#)
798 [nitrogen-oxygen and hydrogen-oxygen isotopes. J. Hazard. Mater., 141181.](#)

带格式的: 缩进: 左侧: 0 厘米, 悬挂缩进: 3.2 字符, 不调整西文与中文之间的空格, 不调整中文和数字之间的空格

设置了格式: 字体: (中文) + 中文正文 (等线), 字体颜色: 自动设置